

Methods

Behavioral tests and animal care were conducted in accordance with the standard ethical guidelines (European Communities Directive 86/609 EEC; National Institutes of Health 1995) and approved by the local ethical committee (CEEA-IMAS-UPF). All experiments were carried out under blind conditions.

Water maze

Animals were habituated to environmental conditions for 15 days and handled by the experimenter daily 4 days before the initiation of the experimental procedures. During the experimental phase, mice were group housed (3-4 mice per cage) under a 12:12-h light-dark schedule (lights on at 0800) in controlled environmental conditions of humidity (60%) and temperature (22 ± 2 °C) with free access to food and water. Only males (6-8 months of age) were tested in this study. All behavioral testing was conducted by the same experimenters in an isolated room and at the same time of the day (08:30 to 15:30). The pool was situated in a 10 m² room with extra maze cues (doors, posters, cabinets, and electrical fixtures) visible from inside the pool (170 cm diameter, depth 60 cm; Panlab S.L., Barcelona). The swimming pool was filled with water (23 ± 1 °C) made opaque with non-toxic white painting (Abacus S.L., Barcelona) and a platform (15 cm diameter) was placed 1.5 cm below the water surface. Diffuse illumination was provided by indirect lighting from 40 W lamps aimed towards the ceiling. Behavioral experimenters were blind to the genotype of the animal.

Two different experimental paradigms were applied. One used general procedures described in detail elsewhere [1], except as noted below. The other was a repeated acquisition paradigm to separately assess working and reference memory. The experiments were performed in two subsequent phases using two separate groups of animals. Two pre-training sessions, in which animals learned the opportunity to escape (the platform) was used in both experiments. Once mice were familiarized with the set-up and acquired procedural learning in the pretraining sessions, the water maze task was performed. The visuo-spatial water maze protocol (Experiment I) consisted of five tasks (2 pre-training, 10 acquisition, 1 probe, 1 cue and 3 reversal sessions) [1,2]. Mice were tested for place learning acquisition in the water maze pool over 10 acquisition sessions (four trials per session; one session per day). The platform was placed in a fixed position in the center of the north-west quadrant and in each trial, mice were placed at one of the starting locations in random order [north, south, east, west (N, S, E, W), including permutations of the four starting points per session] of the swimming pool. Mice were allowed to swim until they located the submerged platform in a fixed position (NW quadrant, 22 cm away from the wall) or until 60 s had elapsed and were then placed on it for 20 s. In the probe session [four trials entering the pool from the four different starting points (N, S, E and W)] the platform was removed and mice were allowed to swim for 60 s without platform. The time spent in the trained and non-trained quadrants during 60 s were recorded. In the cued learning session [four trials entering the pool from the four different starting points (N, S, E and W)] the platform was elevated 1 cm above the water and its position was clearly indicated by a visible cue (black flag) and white curtains prevented the use of extra-maze cues. On the next day, mice performed the reversal learning session [four trials entering the pool from the four different starting points (N, S, E and W), three consecutive acquisition days]. In this test, the platform position was changed to the quadrant opposite to the previous location of the platform (SE). Mice unable to find the platform within 60 s were placed on it for 20 s.

Animals were tested in a repeated reversal learning paradigm (Experiment II) specifically designed to assess short and long-term memories [3,4]. It consisted of eight pairs of acquisition sessions, with the platform hidden, and from one daily session to the next, the platform was placed in a different location (E, SW, center and NW), each position being used once every four consecutive sessions. Each of the four starting positions (N, S, E, W) was used randomly in every daily session. Thus, mice randomly started from each of the four starting positions on the first (odd) trial of a pair and from the same starting position on the second (even) trial of the pair. The first trial of a pair was terminated when the mouse located the platform or when 60 s had elapsed; following a period of 20 s, in which the animal was allowed to stay on the platform. The second trial of a pair was run immediately. Several fixed extra maze cues were constantly visible from the pool. Acquisition and cued sessions consisted of four pairs of trials 30-45 min apart.

In both Experiment I and II, escape latencies, length of the swimming paths and swimming speed for each animal and trial were monitored and computed by a tracking system (SMART, Panlab S.A.) connected to a video camera placed above the pool. To better evaluate the spatial distribution of the behavior of the mice, the paths traveled in peripheral (15 cm wide) and central rings were measured in each trial and the Wishaw's index was calculated, corresponding to the percentage of path traveled within a straight corridor connecting the start and the goal.

Statistical analysis of water maze data was performed by using One-way ANOVA when significant ($P < 0.05$) interaction between factors was found. Acquisition sessions were analysed also with Repeated Measures test (General Linear Model). The dependent variables analyzed in the water maze were escape latencies, length of swimming paths (in the center, periphery and total) and swimming speeds. Data are reported as mean \pm SEM. The statistical analysis was performed using the SPSS 12.0 software.

Active avoidance procedure and object recognition task

Mice were initially housed five per cage in a temperature ($21\pm 1^\circ\text{C}$) and humidity ($65\pm 10\%$) controlled room with a 12-/12- h light/dark cycle (lights on from 08:00 to 20:00 hours) with ad libitum food and water. Experiments took place during the light phase. Mice were trained to avoid an aversive unconditioned stimulus (US), an electric shock (0.2 mA) continuously applied to the grid of the floor, associated with the presentation of a light (10 W) serving as a conditioned stimulus (CS) in a two-way shuttle box apparatus (Panlab, Barcelona). The apparatus consists of a box with two compartments (20×10 cm) connected by a 3×3 cm door. The CS was switched on in the compartment in which the mouse was placed preceding 5 s the onset of the US and overlapping it for 25 s. Using this procedure, the light was presented in the compartment for 30 s (5 s alone and 25 s together with the US). At the end of the 30 s period, both CS and US were automatically turned off. A conditioned response was recorded when the animal avoided the US by changing from the compartment where the animal received the CS into the opposite compartment within the 5 s after the onset of the CS. If animals failed to avoid the shock, they could escape it by crossing during the US (25 s). Between each trial session, there was an intertrial interval of 30 s. The ratio of conditioned with respect to the total number of changes of compartment was also determined. Mice were placed in the shuttle box for 10 min before the start of each session to allow them to explore the box. After this habituation period, mice were subjected daily to 100-trial active avoidance sessions during 10 days.

The object recognition task was performed as reported previously [5] in a plexiglas open-field box (51 cm wide \times 51 cm long \times 58 cm high) with white vertical walls and a white floor divided into 25 equal squares. The light intensity in the middle of the field was 30 lux. The objects to be discriminated were a marble (5.5 cm high, object A) and a plastic (4.5 cm high, object B) figure. First, mice were individually habituated to the open-field for 50 min. The next day, they were submitted to a 10-min acquisition trial (first trial) during which they were placed in the open-field in the presence of object A. Locomotor activity (number of squares crossed), rearings and time that animal took to explore object A (animal's snout directed toward the object at a distance < 1 cm) were recorded. A 10-min retention trial (second trial) occurred 1 h later. During this second trial, objects A and B were placed in the open-field, and locomotor activity, rearings and time that animal took to explore object A (t_A) and object B (t_B) were recorded. A recognition index was defined as $[t_B/(t_A + t_B)] \times 100$.

For the active avoidance paradigm, differences in the number of conditioned changes and in the ratio of conditioned versus total changes were analysed using Two-way ANOVA (day as within subjects factor, genotype as between subjects factor). For the object recognition task, number of squares crossed and rears were analysed using Two-way ANOVA (trial as within subjects factor, genotype as between subjects factor). Comparisons between genotypes were by One-way ANOVA and the Bonferroni post-test. In the object recognition task, recognition index of the different groups were compared using One-way ANOVA. Analyses were conducted using the statistical package SPSS 13.0. Differences were considered significant when the probability of error was less than 5%. Data are expressed as mean \pm SEM.

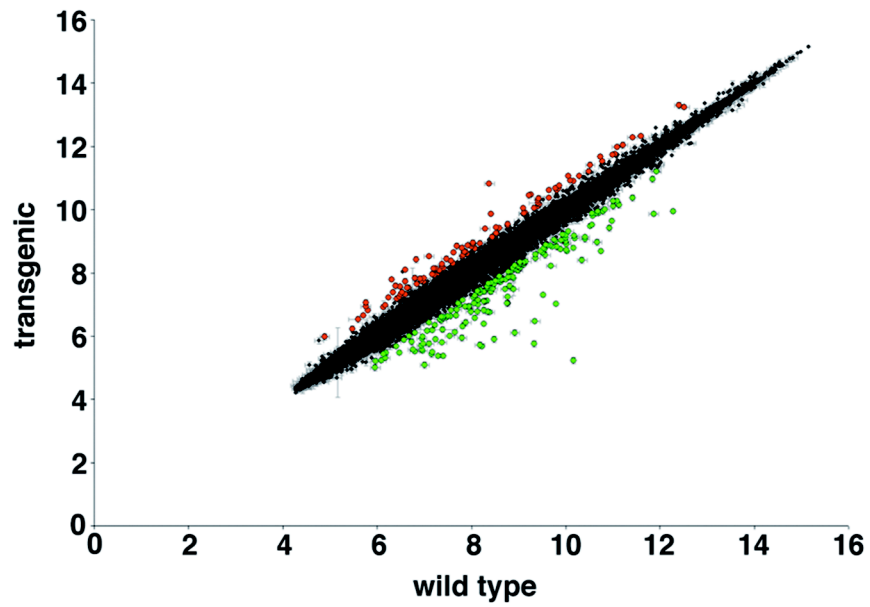
Electrophysiology in vitro

Transgenic and wild type littermates were anaesthetised by intraperitoneal injection of a mixture of medetomidine (1 mg/kg) and ketamine (76 mg/kg), before being killed by cervical dislocation. The brains were rapidly removed and chilled ($< 3^\circ\text{C}$), in oxygenated, ice-cold cutting solution composed of (in mM): 110 choline chloride, 2.5 KCl, 1.25 NaH_2PO_4 , 25 NaHCO_3 , 0.5 CaCl_2 , 7 MgCl_2 , 1.3 ascorbate, 3 pyruvate, and 7 dextrose. Parasagittal slices were cut from the dorsal hippocampus using a Vibroslice (Campden Instruments, Loughborough, UK). Slices were maintained in standard artificial cerebrospinal fluid (ACSF) consisting of (in mM): 125 NaCl, 26 NaHCO_3 , 3 KCl, 2 CaCl_2 , 1.0 MgCl_2 , 1.25 NaH_2PO_4 , and 10 glucose and gassed with 95% O_2 -5% CO_2 during the whole process. Extracellular experiments used 400 μm thick slices prepared from 5-6 month old mice, and maintained in an interface chamber kept at 33°C , and micropipettes filled with ACSF (4-5 $\text{M}\Omega$). Granule cell responses were evoked with a bipolar Nichrome wire stimulating electrode placed in molecular layer 50-200 μm from the recording site in granular layer. Single pulse stimuli were used to construct a stimulus response curve to identify the stimulus strength needed to evoke population spikes of half maximum amplitude, which were then used to perform a paired-pulse facilitation/inhibition experiment. Whole cell recordings used 300 μm thick slices prepared from 1-2 month old mice and maintained submerged at 31 - 33°C , under an Olympus BX-51 DIC microscope with water-immersion objectives, for patch-clamp recordings in whole-cell configuration under voltage clamp. Patch pipettes contained (in mM): cesium gluconate, 145; CsCl, 10; HEPES, 10; NaCl, 2; and EGTA, 0.1; pH = 7.25 (adjusted with CsOH). Granule cell bodies were selected for recording according to their size, location and appearance. A bipolar stimulating electrode was placed at perforant path 70-280 μm from the granular cell layer. Constant current pulses were delivered to perform an input-output curve. Evoked IPSCs were measured as the integral of the membrane current response, which estimates charge transfer. Spontaneous IPSCs were identified and measured using MiniAnalysis software (Synaptosoft Inc).

References

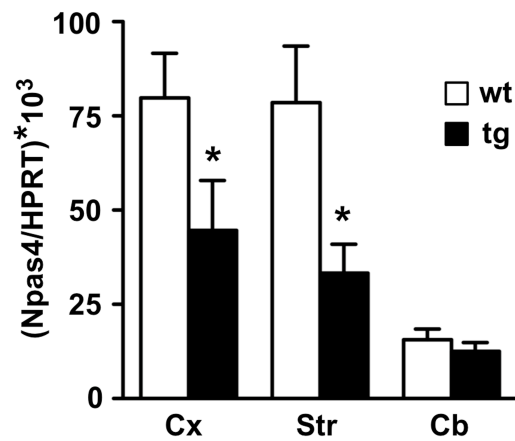
1. Morris R (1984) Developments of a water-maze procedure for studying spatial learning in the rat. *J Neurosci Methods* 11 (1):47-60. doi:0165-0270(84)90007-4 [pii]
2. Chen G, Chen KS, Knox J, Inglis J, Bernard A, Martin SJ, Justice A, McConlogue L, Games D, Freedman SB, Morris RG (2000) A learning deficit related to age and beta-amyloid plaques in a mouse model of Alzheimer's disease. *Nature* 408 (6815):975-979. doi:10.1038/35050103
3. van der Staay FJ, de Jonge M (1993) Effects of age on water escape behavior and on repeated acquisition in rats. *Behav Neural Biol* 60 (1):33-41
4. Escorihuela RM, Vallina IF, Martinez-Cue C, Baamonde C, Dierssen M, Tobena A, Florez J, Fernandez-Teruel A (1998) Impaired short- and long-term memory in Ts65Dn mice, a model for Down syndrome. *Neurosci Lett* 247 (2-3):171-174
5. Meziane H, Dodart JC, Mathis C, Little S, Clemens J, Paul SM, Ungerer A (1998) Memory-enhancing effects of secreted forms of the beta-amyloid precursor protein in normal and amnesic mice. *Proc Natl Acad Sci U S A* 95 (21):12683-12688

Figure S1



Statistical values and scatter plot of all probes contained in the genome-wide analysis. Spots with $|\text{Fold Change}| > 1.6$ and $\text{FDR} < 0.1$ are highlighted in green (repressed genes) and red (induced genes).

Figure S2



Real-time qPCR analysis of Npas4. Expression levels of Npas4 mRNA in cerebral cortex (Cx), striatum (Str) and cerebellum (Cb) from wild type (wt) and transgenic (tg) mice. Values are normalized with respect to HPRT mRNA content. Results are the mean \pm SEM of 8-12 mice in two separate experiments * $P < 0.05$ (two-tailed, unpaired t -test).

Figure S3

A Npas4

CTCCCTCTCCCGTTTCGACGTCA^{CGGGA}FGACGTC
GGAAGTCTGGGAGGGAGGAGGAGCACCCCCCT
CCCCAGC^{CAGT}GGCTCCCTCTGCAGCTTGCTTTA
GCCCAGCCTCCCGCCTCCCGCTGCCCCCCCCGT
CTCTAAAAACGAGCCCCCACGCCTGTCA^{GGAGC}
TATATA^{GGCGGATCGAGGCAGGGCAGGGGGGC}
AGCGCTGCCGAGCGGAGCCCAGGAGTGGAGCG
AGAGCGAGCAAGAGCCTGAGCGAAAAGACCGGG
AAGCAAGGAAGAGGAAGCCTCCGGTGCATCGGG
AAAGGATCGCAGGTGCTCGGGAGCCGGAGCTGG
AGCTCCACAGCCGGCA^{GTCATG}TACCGATCCACC

B c-fos

GTTGAAAGCCTGGGGCGTAGAGT^{TGAC}GACAGAGC
GCCCCGAGAGGGCCTTGGGGCGCGCTTCCCCCCCC
TTCCAGTTCCGCCAG^{TGAC}GTAGGAAGTCCATCCAT
TCACAGCGCTTC^{TATAAA}GGCGCCAGCTGAGGCGCC
TACTACTCCAACCGCG^{ACTG}CAGCGAGCA^{ACTG}AGA
AG^{ACTG}GATAGAGCCGGCGTTCCGCGAACGAGCA
G^{TGAC}CGCGCTCCCACCCAGCTCTGCTCTGCAGCTC
CCACCAGTGTCTACCCCTGGACCCCTTGCCTGGCTT
TCCCCAACTTCGACC^{ATGATG}TTCTCGGGTTTCAAC
GCCGACTACGAGGC^{GTCAT}TCTCCCGCTGCAGTAGC

C BDNF exon IV

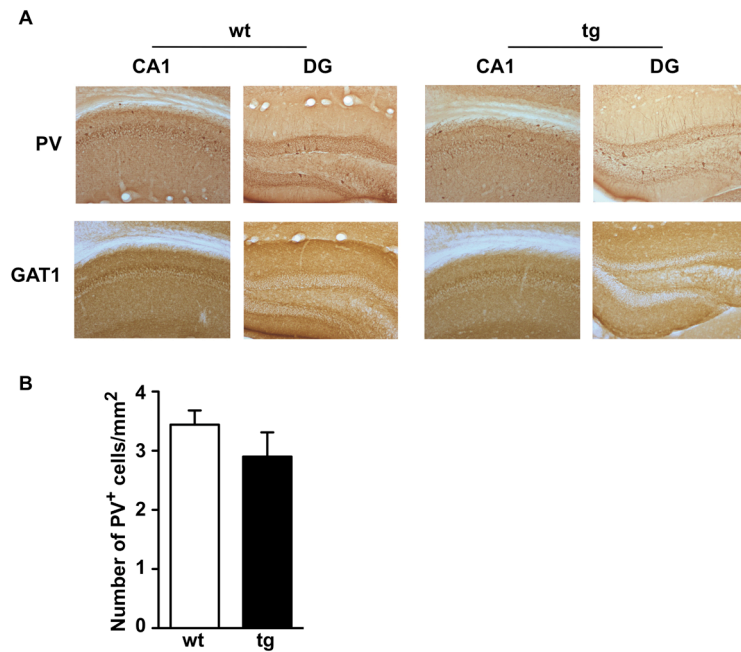
CGTGCACTAGAGTGTCTATTTTCGAGGCAGAGGAGGT
ATCATATGACAGCTCAC^{GTCAT}AGGCAGCGTGGAGCC
CTCTCGTGGACTCCCACCCACTTCCCATTACCGAG
GAGAGGACTGCTCTCGCTGCCGCTCCCCCACCCAC
CCCCGGCGAGCTAGCATGAAATCTCCCAGCCTCTGC
CTAGATCAAATGGAGCTTCTCGCTGAAGGCGTGCGA
GTATTACCTCCGCCATGCAATTTCCACTATCAATAATT
AACTTCTTTGCTGCAGAACAGGAGTACATATCGGCCA
CCAAAGACTCGCCCCCTCCCCCTTTAACTGAAGAGA
AGGGGAAATATATAGTAAGAGTCTAGAACCTTGGGGA
CCGGTCTTCCCAGAGCAGCTGCCTTGATGTTACTT
^{TGAC}AAAGTAG^{TGAC}TGAAAAAG

D DREAM

ACTGGAGGTT^{GTCAT}GGATGGAGGCGAAGGAGGGG
GGAGATAAGAGGGGGAGGGAAGAGGCAGAGGAAG
AGAGGTGGAGCTAAGACTCGGAAGGAAGGGAGGGT
GGAAGGAGTGGGCAGGGGGCGGGAGAGAAACCTC
CAG^{TGAC}AATTGCGTCTGGGTCCAAGCAAACATGAG
GCAGCTGCCAGCCGGACCAAGCAGTCTGGCTTGCT
CGGGCTGCAAAGCGGGAAGATTAG^{TGAC}GGTCCCT
TTCAGCAGCAGAG^{ATG}CAGAGGACCAAGGTAGGCG
CTG

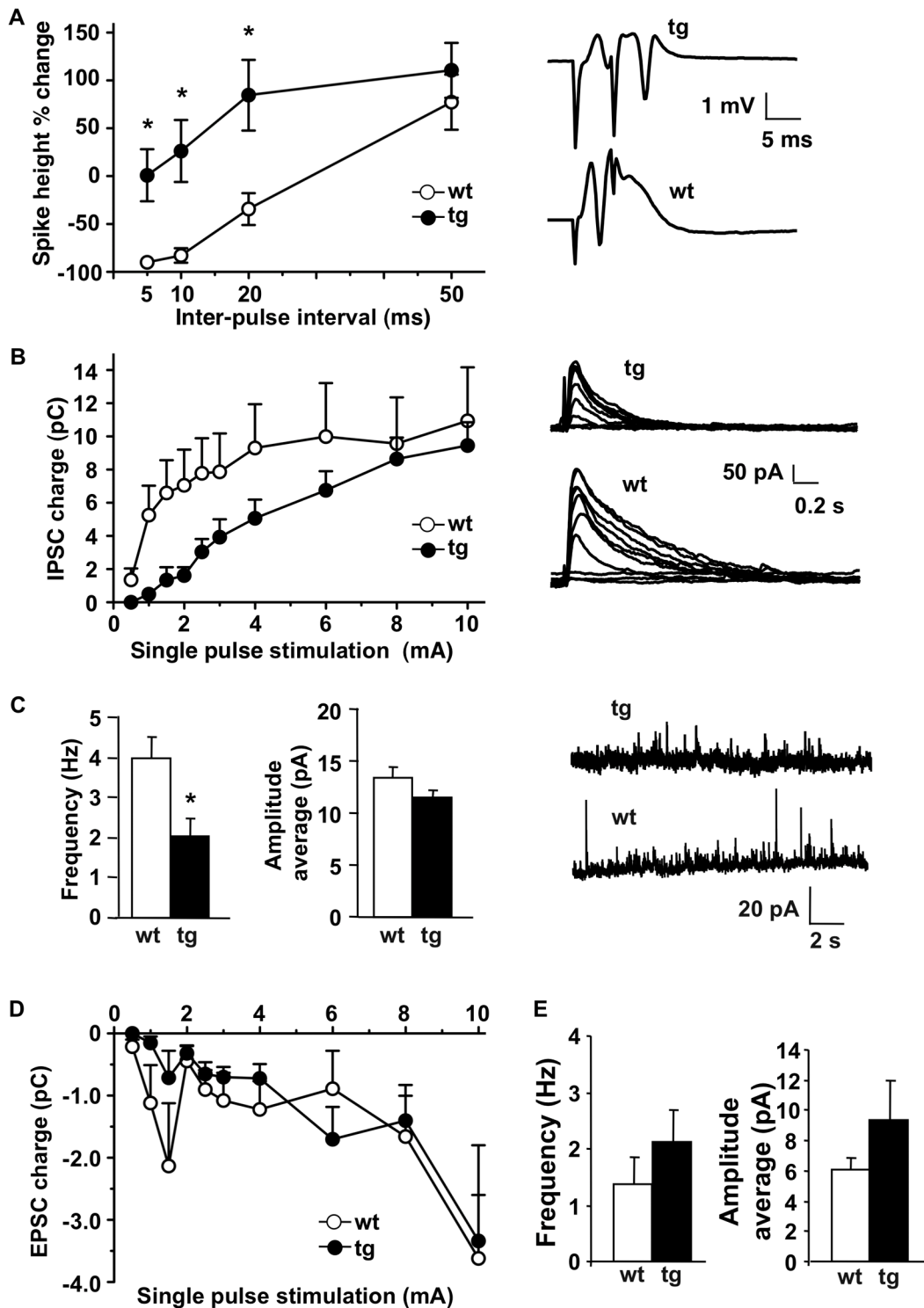
Nucleotide sequence of mouse promoters. (A) Npas4, (B) c-fos, (C) BDNF exon IV and (D) DREAM gene regulatory regions. The TATA box (blue), the translation start site (green) and the location of putative DRE sites (red) are indicated.

Figure S4



Total GABAergic cellularity is not modified in transgenic hippocampus. (A) Coronal sections from wild type (wt) and transgenic (tg) hippocampus showing immunostained parvalbumin (PV) positive cells and total GAT1 immunoreactivity in CA1 and dentate gyrus (DG). Bar represents 100 μ m. **(B)** Quantification of parvalbumin positive cells in wild type and transgenic hippocampus.

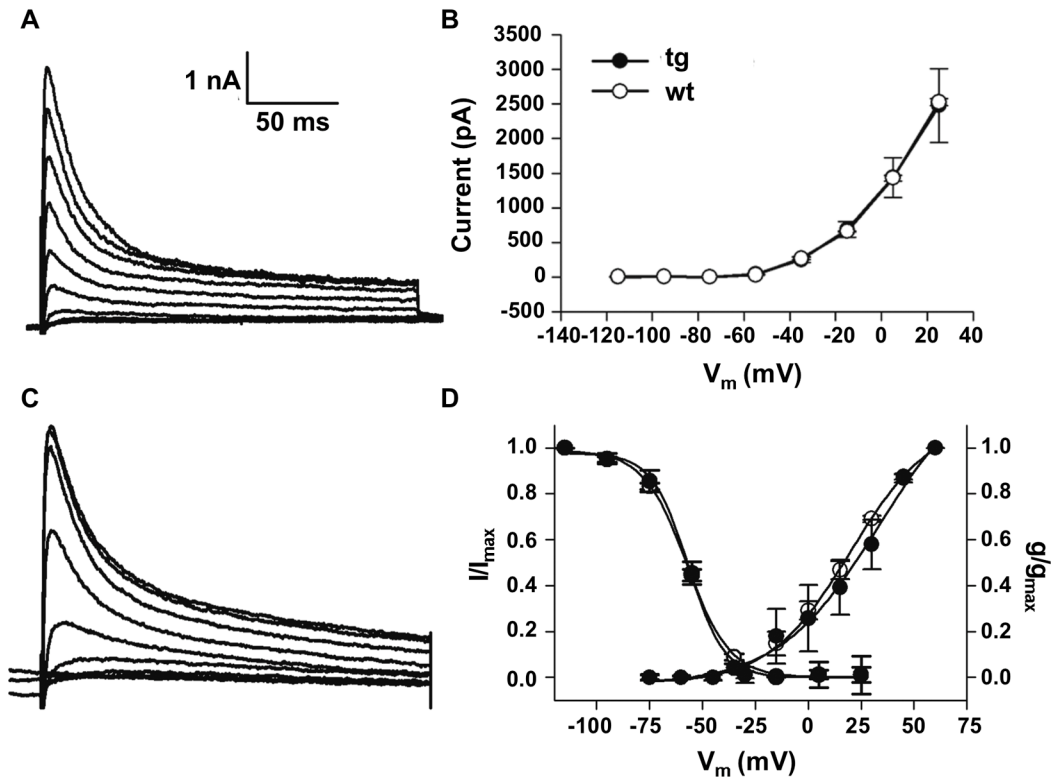
Figure S5



In vitro depressed inhibition in dentate gyrus of transgenic mice. (A) Effect of the interval between paired stimuli on the difference in population spike amplitude as percentage of the first response. The stimulus intensity required for half-maximal population spike with single stimuli was not different between genotypes (wt 8.2 ± 1.4 V, tg 10.9 ± 1.6 V). Paired evoked responses at 5 ms inter-stimulus interval shows

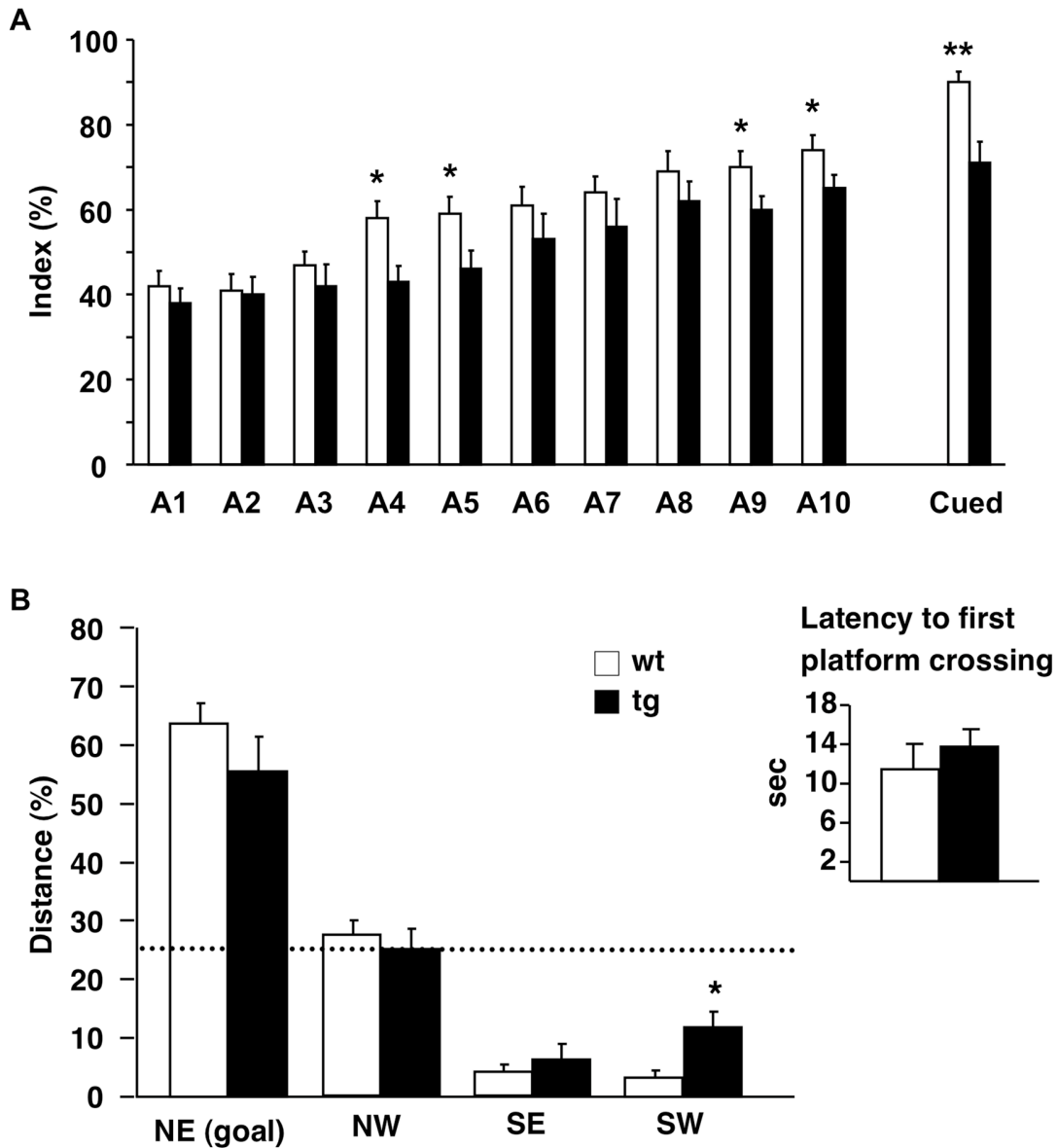
inhibition in wt (n=13) and facilitation in tg (n=17) mice (Two-way ANOVA with Bonferroni post-test, * $P < 0.05$). At right are original traces of population spikes in pyramidal cells at 5 ms inter-pulse interval showing the inhibition and facilitation in wt and tg mice, respectively. **(B)** Inhibitory postsynaptic currents (IPSCs) evoked by single pulse stimulation at 0 mV holding potential in whole-cell recordings. Charge transferred during IPSC as a function of stimulus strength shows decreased inhibitory current in tg mice (n=13) compared to wt (n=26). Mean IPSC area difference is significant at the 0.05 level (Univariate ANOVA with Bonferroni post-test). At right are superimposed IPSCs evoked by stimuli in the range 0.5 to 10 mA. **(C)** Frequency and average amplitude of spontaneous IPSCs in wt (n = 12) and tg (n = 10) mice recorded at 0 mV (Mann-Whitney Rank Test, * $P < 0.05$). At right are representative traces of spontaneous IPSCs. **(D)** Excitatory postsynaptic currents (EPSCs) evoked by single pulse stimulation at -80 mV holding potential in whole-cell recordings. Charge transferred during EPSC as a function of stimulus strength shows no difference (Univariate ANOVA) in excitatory currents between genotypes (wt n=26, tg n=14). **(E)** Frequency and average amplitude of spontaneous EPSCs recorded at -80 mV shows no difference (Mann-Whitney Rank Test) between genotypes (wt n = 10, tg n = 11). Vertical error bars represent SEM.

Figure S6



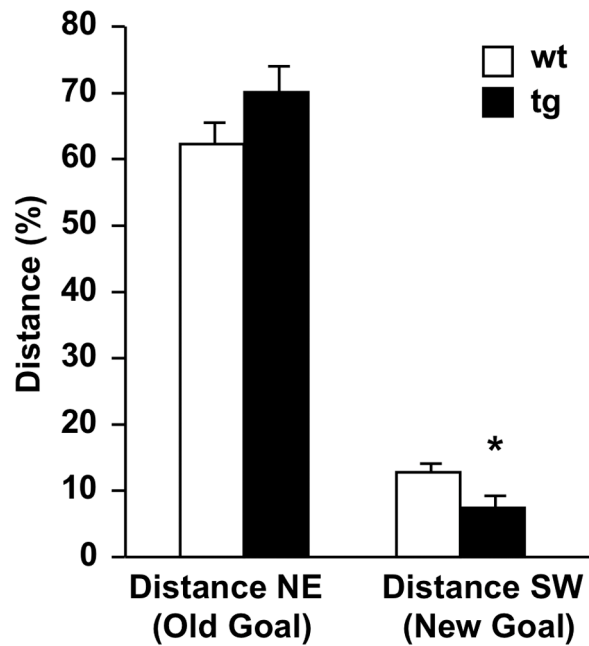
A-type current is not altered in daDREAM mice. (A) A-current recorded in hippocampal neurons in wild type mice. (B) Pooled data showing that peak amplitude of A-type current at different voltage steps is similar in wild-type (wt) and transgenic (tg) mice. (C) Typical traces showing the steady-state inactivation of A-type current in wild type mice. Currents were recorded during membrane potential held to 30 mV following a 400 ms conditioning pulse from -115 mV to +25 mV with 20 mV steps. (D) Steady-state activation and inactivation curves in transgenic and wild type mice. The data were fitted with Boltzmann function. Steady-state activation is plotted as voltage steps versus g/g_{max} , while the steady-state inactivation is plotted as voltage steps versus I/I_{max} .

Figure S7



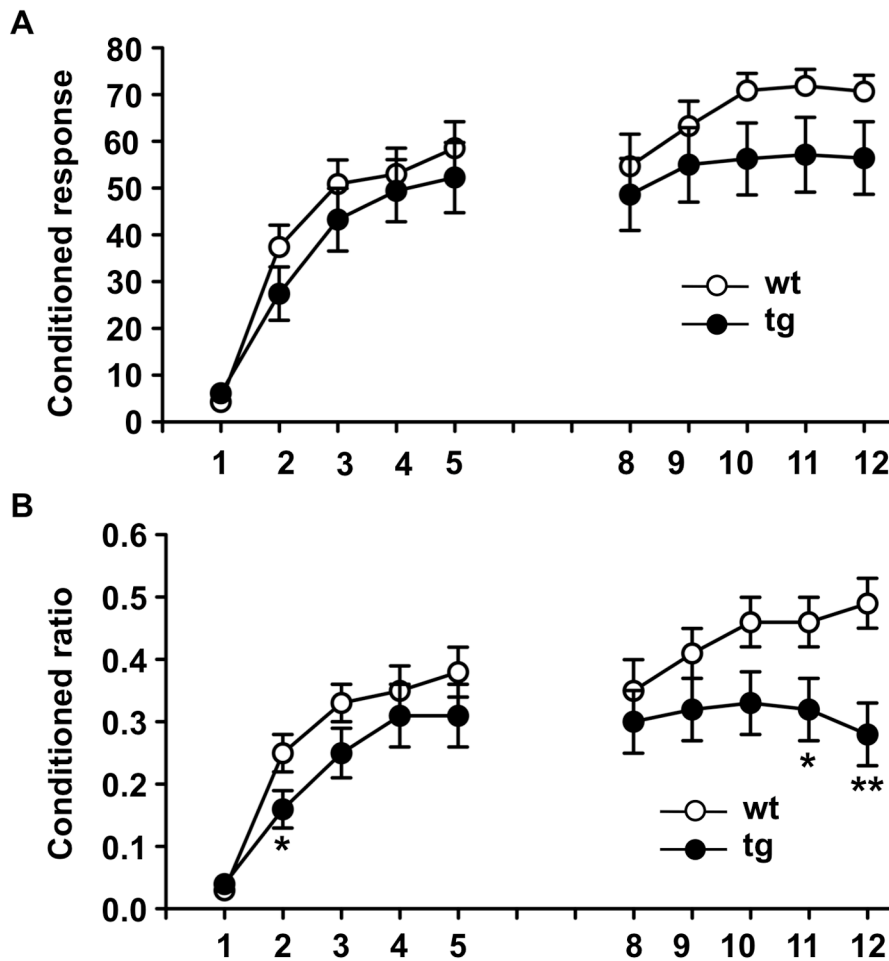
Impaired Wishaw index in the water maze in daDREAM mice. (A) Wishaw index, defined as % path inside the optimal corridor to reach the platform, indicates the use of less efficient learning strategies in transgenic (tg) than in wild type (wt) littermates across acquisition sessions (Repeated measures ANOVA $F_{(1,19)} = 10.314$, $P = 0.003$). * $P < 0.05$; ** $P < 0.01$. (B) No differences in permanence time in trained quadrant (NE) or the first platform cross latency (inset) were observed between transgenic and wild type mice in the removal session, which assesses reference memory through mice preference for the previously trained quadrant. Data are expressed as mean \pm SEM.

Figure S8



Impaired performance in the reversal session of the water maze in daDREAM mice. In the reversal-learning test, the platform was hidden in the opposite quadrant to the trained one. Transgenic (tg) mice showed a non-significant trend to search more the platform in the old-goal quadrant and spent less time in the new-goal quadrant than wild type (wt) mice (One-way ANOVA $F_{(1,19)} = 5.610$, $P = 0.029$). Data are expressed as mean \pm SEM. * $P < 0.05$.

Figure S9



Reduced learning in the active avoidance procedure. (A) Repeated measures ANOVA for conditioned changes revealed no significant main effect in transgenic (tg) mice. (B) Repeated measures ANOVA for the ratio of conditioned changes, with respect to the total number of changes of compartment, revealed a significant main effect of day of training ($F_{(9,288)} = 45.851, P < 0.001$), genotype ($F_{(2,32)} = 4.633, P < 0.05$) and interaction between these two factors ($F_{(18,288)} = 2.545, P < 0.01$). Post-hoc comparisons following significant one-way ANOVA for each day of training showed that tg mice significantly decreased the ratio of conditioned changes with respect to wild type (wt) mice on day 2 and on the last two sessions. Data are shown as mean \pm SEM in 100 trial sessions during 12 days (wt, $n = 15$; tg, $n = 11$). * $P < 0.05$, ** $P < 0.01$ (Bonferroni post-test).

Table S1 Sequences of primers and probes used for real-time quantitative PCR

transcript	primer	5'-3' sequence	MGB probe 5'-3' sequence
DREAM	5'	cacctatgcacacttctcttca	FAM-tgccttcgatgctgat
	3'	accacaaaagtcctcaaagtggat	
daDREAM	5'	cacctatgcacacttctcttca	VIC-cgcctttgctgcggc
	3'	accacaaaagtcctcaaagtggat	
GABAR α 2	5'	aagacaaaattgagcacatgcaa	FAM-caagcagcagagaccata
	3'	tgggtcccacaccagaaga	
BDNF	5'	cgagtgggtcacagcggcaga	none ^a
	3'	cgaacatacgattgggtagtt	
GABAR β 2	5'	ccattctctctgggtctcctt	none
	3'	tgattgtggtcattgttaggacagt	
GABAR β 3	5'	ccttctggatcaattacgatgca	none
	3'	tgagtgttgatggttgcacatggt	
PSD95	5'	gtttggatcctgtgtccctcat	none
	3'	ggtaatcgcggccgtctat	
β -actin	5'	gtcatcactattggcaacgag	FAM-tccatcatgaagtgtgacgttgaca
	3'	gacctctatgccaacacagt	
HPRT	5'	tggatacaggccagactttgt	FAM-ttgaattccagacaagttt
	3'	ctgaagtactcattatagtcagggcata	

^aSYBR Green based qPCR

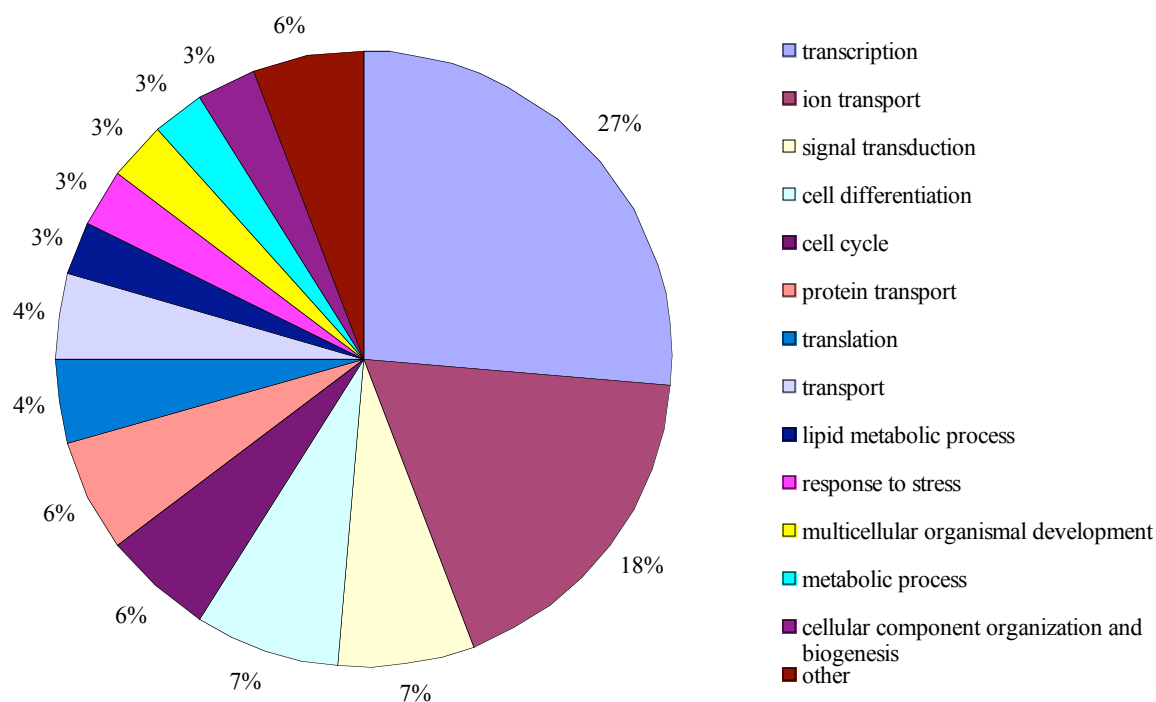
Table S2 Assays from Applied Biosystems used for real-time quantitative PCR

Transcript	Assay ID
Npas4	Mm00463644_m1
Nr4a1	Mm011300401_m1
c-Fos	Mm00487425_m1
Mef2c	Mm01340839_m1
Per3	Mm00478120_m1
JunB	Mm00492781_m1
Sox11	Mm01281943_s1
Egr2	Mm00456650_m1
Mbd4	Mm01184338_m1
GABAR α 1	Mm01299033_m1
GAT1	Mm00618601_m1
VIAAT	Mm00494138_m1
GAD2	Mm00484623_m1
KChIP1	Mm01189526_m1
KChIP2	Mm00518914_m1
KChIP4	Mm00518835_m1
CREB	Mm01342452-m1

Table S3 Sequences of primers used for semiquantitative PCR

Transcript	primer	5'- 3' sequence
Npas4	5'	cctctcccgttcgacgtcac
	3'	ggcagcagctccttgaggttc
c-fos	5'	ctacacgcggaaggctaggag
	3'	cagtcgcggttgagtagtagg
BDNF exon IV	5'	aatgcgcggaattctgattctg
	3'	ggggagggggcgagtcttt
DREAM	5'	tgagaggccaggactaggagca
	3'	agcgcctaccttggtcctctg

Table S4 Genes whose expression levels are modified in transgenic compared to wild type hippocampus. Clustering according to Gene Ontology (Biological process)

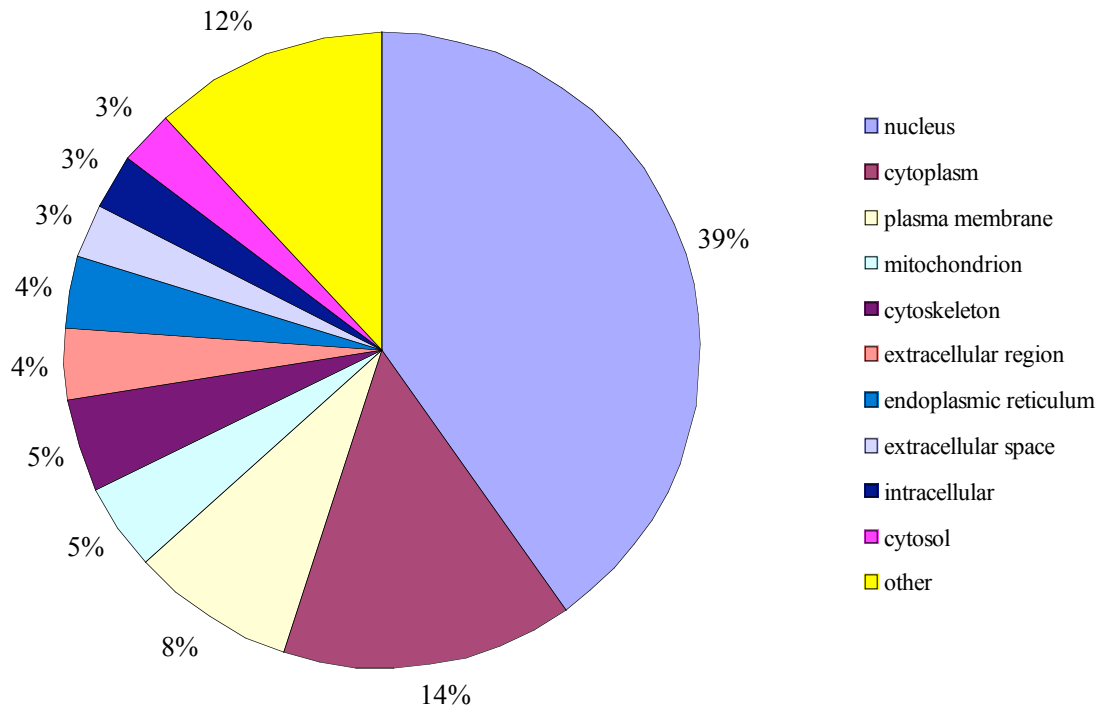


Probe Set ID	Gen Symbol	Gene Name	Change
Category: transcription			
1415899_at	Junb	Jun-B oncogene	DOWN
1416250_at 1448272_at	Btg2	B-cell translocation gene 2, anti-proliferative	DOWN
1416505_at	Nr4a1	nuclear receptor subfamily 4, group A, member 1	DOWN
1418174_at 1438211_s_at	Dbp	D site albumin promoter binding protein	DOWN
1419380_at	Zfp423	zinc finger protein 423	DOWN
1421028_a_at 1451507_at	Mef2c	myocyte enhancer factor 2C	DOWN
1421087_at	Per3	period homolog 3 (Drosophila)	DOWN
1421163_a_at	Nfia	nuclear factor I/A	DOWN
1427682_a_at	Egr2	early growth response 2	DOWN
1439998_at	Jmjd1c	jumonji domain containing 1C	DOWN
1441573_at	Scmh1	Sex comb on midleg homolog 1	DOWN
1443020_at	Hmbox1	homeobox containing 1	DOWN
1449578_at	Supt16h	suppressor of Ty 16 homolog (S. cerevisiae)	DOWN
1455246_at	Smarcc1	SWI/SNF related, matrix associated, actin dependent regulator of chromatin, subfamily c, member 1	DOWN
1459250_at	Tshz2	teashirt zinc finger family member 2	DOWN

1459372_at	Npas4	neuronal PAS domain protein 4	DOWN
1429951_at	Ssbp2	single-stranded DNA binding protein 2	UP
1448406_at	Eid1	EP300 interacting inhibitor of differentiation 1	UP
Category: ion transport			
1421738_at	Gabra2 /// LOC100047443	gamma-aminobutyric acid (GABA-A) receptor, subunit alpha 2 /// similar to Gamma-aminobutyric-acid receptor subunit alpha-2 precursor (GABA(A) receptor subunit alpha-2)	DOWN
1430485_at	Trpc2	transient receptor potential cation channel, subfamily C, member 2	DOWN
1436239_at	Slc5a5	solute carrier family 5 (sodium iodide symporter), member 5	DOWN
1439987_at	Grik1	glutamate receptor, ionotropic, kainate 1	DOWN
1443865_at 1455444_at	Gabra2	gamma-aminobutyric acid (GABA-A) receptor, subunit alpha 2	DOWN
1449421_a_at	Kcne2	potassium voltage-gated channel, Isk-related subfamily, gene 2	DOWN
1450712_at	Kcnj9	potassium inwardly-rectifying channel, subfamily J, member 9	DOWN
1455136_at	Atp1a2	ATPase, Na ⁺ /K ⁺ transporting, alpha 2 polypeptide	DOWN
1436994_a_at	Hist1h1c	histone cluster 1, H1c	UP
1440397_at	Cacna2d1	calcium channel, voltage-dependent, alpha2/delta subunit 1	UP
1442742_at	Atp2c1	ATPase, Ca ⁺⁺ -sequestering	UP
1456923_at	Trpm3	transient receptor potential cation channel, subfamily M, member 3	UP
Category: signal transduction			
1417432_a_at 1454696_at	Gnb1	guanine nucleotide binding protein (G protein), beta 1	DOWN
1421385_a_at	Myo7a	myosin VIIa	DOWN
1439843_at 1441974_at	Camk4	calcium/calmodulin-dependent protein kinase IV	DOWN
1440801_s_at	Adrbk2	adrenergic receptor kinase, beta 2	DOWN
1454770_at	Cckbr	cholecystokinin B receptor	DOWN
Category: cell differentiation			
1416953_at	Ctgf	connective tissue growth factor	DOWN
1423477_at	LOC100044533 /// Zic1	similar to Zic protein /// zinc finger protein of the cerebellum 1	UP
1437904_at	Rbm45	RNA binding motif protein 45	UP
1438936_s_at 1438937_x_at	Ang	angiogenin, ribonuclease, RNase A family, 5	UP
1439627_at	Zic1	zinc finger protein of the cerebellum 1	UP
Category: cell cycle			
1448229_s_at	Ccnd2	cyclin D2	DOWN
1448830_at	Dusp1	dual specificity phosphatase 1	DOWN
1430811_a_at	Nuf2	NUF2, NDC80 kinetochore complex component, homolog (S. cerevisiae)	UP
1437579_at	Nek2	NIMA (never in mitosis gene a)-related expressed kinase 2	UP
Category: protein transport			
1444037_at	Lman1	lectin, mannose-binding, 1	DOWN
1449859_at	Golt1b	golgi transport 1 homolog B (S. cerevisiae)	DOWN
1418898_at 1423322_at 1449262_s_at 1450937_at	Lin7c	lin-7 homolog C (C. elegans)	UP

1457969_at	Rabif	RAB interacting factor	UP
Category: translation			
1455600_at	Rps3	ribosomal protein S3	DOWN
1431006_at	Mrpl3	mitochondrial ribosomal protein L3	UP
1434624_x_at	Rps9	ribosomal protein S9	UP
Category: transport			
1456187_at	Slc7a14	solute carrier family 7 (cationic amino acid transporter, y+ system), member 14	DOWN
1458203_at	Spire1	Spire homolog 1 (Drosophila)	DOWN
1450779_at	Fabp7	fatty acid binding protein 7, brain	UP
Category: lipid metabolic process			
1443904_at	Fads6	fatty acid desaturase domain family, member 6	DOWN
1415904_at 1431056_a_at	Lpl	lipoprotein lipase	UP
Category: response to stress			
1429463_at	Prkaa2	protein kinase, AMP-activated, alpha 2 catalytic subunit	DOWN
1431182_at	EG666031 /// Hspa8 /// LOC624853 /// LOC641192	predicted gene, EG666031 /// heat shock protein 8 /// hypothetical LOC624853 /// similar to heat shock protein 8	DOWN
Category: multicellular organismal development			
1418687_at	Arc	activity regulated cytoskeletal-associated protein	DOWN
1419308_at	Invs	inversin	DOWN
Category: metabolic process			
1424877_a_at	Alad /// LOC100046072	aminolevulinate, delta-, dehydratase /// similar to aminolevulinate, delta-, dehydratase	DOWN
1439740_s_at	Uck2	uridine-cytidine kinase 2	UP
Category: cellular component organization and biogenesis			
1435551_at	Fhod3	formin homology 2 domain containing 3	DOWN
1439397_at	Fmn1	formin 1	DOWN
Category: other			
1417765_a_at	Amy1	amylase 1, salivary	DOWN
1424105_a_at 1438390_s_at	Pttg1	pituitary tumor-transforming 1	DOWN
1417461_at 1417462_at	Cap1	CAP, adenylate cyclase-associated protein 1 (yeast)	UP
1417638_at	Lefty1	left right determination factor 1	UP

Table S5 Genes whose expression levels are modified in transgenic compared to wild type hippocampus. Clustering according to Gene Ontology (Cellular Component)



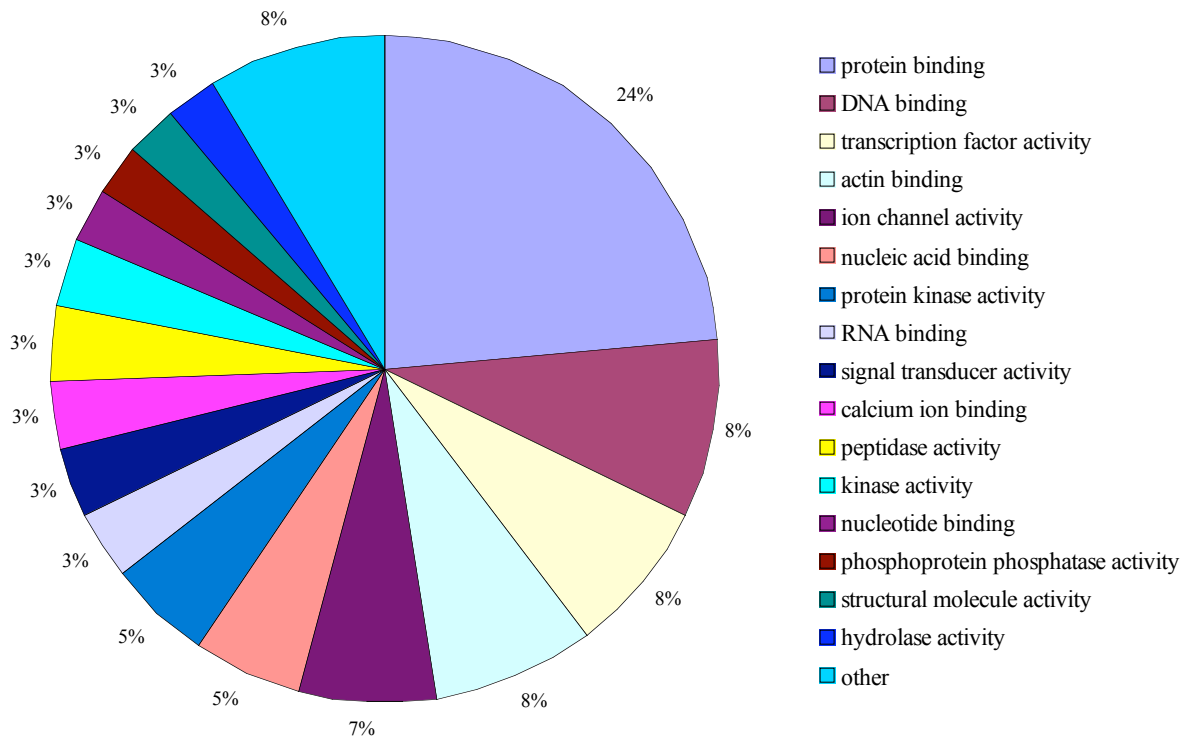
Probe Set ID	Gen Symbol	Gene Name	Change
Category: nucleus			
1415899_at	Junb	Jun-B oncogene	DOWN
1416200_at	Il33	interleukin 33	DOWN
1416505_at	Nr4a1	nuclear receptor subfamily 4, group A, member 1	DOWN
1418174_at 1438211_s_at	Dbp	D site albumin promoter binding protein	DOWN
1419308_at	Invs	inversin	DOWN
1419380_at	Zfp423	zinc finger protein 423	DOWN
1421028_a_at 1451507_at	Mef2c	myocyte enhancer factor 2C	DOWN
1421087_at	Per3	period homolog 3 (Drosophila)	DOWN
1421163_a_at	Nfia	nuclear factor I/A	DOWN
1422659_at 1427763_a_at	Camk2d	calcium/calmodulin-dependent protein kinase II, delta	DOWN
1423100_at	Fos	FBJ osteosarcoma oncogene	DOWN
1424105_a_at 1438390_s_at	Pttg1	pituitary tumor-transforming 1	DOWN
1427682_a_at	Egr2	early growth response 2	DOWN
1429463_at	Prkaa2	protein kinase, AMP-activated, alpha 2 catalytic subunit	DOWN
1431708_a_at	Tia1	cytotoxic granule-associated RNA binding protein 1	DOWN

1437537_at	Casp9	caspase 9	DOWN
1439397_at	Fmn1	formin 1	DOWN
1439843_at 1441974_at	Camk4	calcium/calmodulin-dependent protein kinase IV	DOWN
1439998_at	Jmjd1c	jumonji domain containing 1C	DOWN
1440125_at 1442654_at	A530054K11Rik	RIKEN cDNA A530054K11 gene	DOWN
1441573_at	Scmh1	Sex comb on midleg homolog 1	DOWN
1443020_at	Hmbox1	homeobox containing 1	DOWN
1444092_at	9430025M13Rik	RIKEN cDNA 9430025M13 gene	DOWN
1448229_s_at	Ccnd2	cyclin D2	DOWN
1449490_at	Mbd4	methyl-CpG binding domain protein 4	DOWN
1449578_at	Supt16h	suppressor of Ty 16 homolog (S. cerevisiae)	DOWN
1455246_at	Smarcc1	SWI/SNF related, matrix associated, actin dependent regulator of chromatin, subfamily c, member 1	DOWN
1458240_at	Magi1	Membrane associated guanylate kinase, WW and PDZ domain containing 1	DOWN
1459250_at	Tshz2	teashirt zinc finger family member 2	DOWN
1459372_at	Npas4	neuronal PAS domain protein 4	DOWN
1423477_at	LOC100044533 /// Zic1	similar to Zic protein /// zinc finger protein of the cerebellum 1	UP
1424784_at	OTTMUSG00000010 657	predicted gene, OTTMUSG00000010657	UP
1426906_at 1452231_x_at	Ifi203	interferon activated gene 203	UP
1429308_at	Prdm16	PR domain containing 16	UP
1429951_at	Ssbp2	single-stranded DNA binding protein 2	UP
1430811_a_at	Nuf2	NUF2, NDC80 kinetochore complex component, homolog (S. cerevisiae)	UP
1431057_a_at	Prss23	protease, serine, 23	UP
1434171_at	C330011K17Rik	RIKEN cDNA C330011K17 gene	UP
1436994_a_at	Hist1h1c	histone cluster 1, H1c	UP
1437579_at	Nek2	NIMA (never in mitosis gene a)-related expressed kinase 2	UP
1437904_at	Rbm45	RNA binding motif protein 45	UP
1439627_at	Zic1	zinc finger protein of the cerebellum 1	UP
1448406_at	Eid1	EP300 interacting inhibitor of differentiation 1	UP
1455657_at	2610207I05Rik	RIKEN cDNA 2610207I05 gene	UP
Category: cytoplasm			
1418701_at	Comt1	catechol-O-methyltransferase 1	DOWN
1418726_a_at	Tnnt2	troponin T2, cardiac	DOWN
1431182_at	EG666031 /// Hspa8 /// LOC624853 /// LOC641192	predicted gene, EG666031 /// heat shock protein 8 /// hypothetical LOC624853 /// similar to heat shock protein 8	DOWN
1440142_s_at	Gfap	glial fibrillary acidic protein	DOWN
1449154_at	Col11a1	collagen, type XI, alpha 1	DOWN
1453994_at	C230094A16Rik	RIKEN cDNA C230094A16 gene	DOWN
1455136_at	Atp1a2	ATPase, Na ⁺ transporting, alpha 2 polypeptide	DOWN
1455342_at	A230083H22Rik	RIKEN cDNA A230083H22 gene	DOWN
1417461_at 1417462_at	Cap1	CAP, adenylate cyclase-associated protein 1 (yeast)	UP

1418493_a_at 1436853_a_at	Snca	synuclein, alpha	UP
1425521_at	Paip1	polyadenylate binding protein-interacting protein 1	UP
1427883_a_at	Col3a1	collagen, type III, alpha 1	UP
1430979_a_at	Prdx2	peroxiredoxin 2	UP
1441955_s_at	LOC676674 /// Paip1	similar to poly(A) binding protein interacting protein 1 /// polyadenylate binding protein-interacting protein 1	UP
1446144_at	Pex5l	peroxisomal biogenesis factor 5-like	UP
1450779_at	Fabp7	fatty acid binding protein 7, brain	UP
Category: plasma membrane			
1421738_at	Gabra2 /// LOC100047443	gamma-aminobutyric acid (GABA-A) receptor, subunit alpha 2 /// similar to Gamma-aminobutyric-acid receptor subunit alpha-2 precursor (GABA(A) receptor subunit alpha-2)	DOWN
1436239_at	Slc5a5	solute carrier family 5 (sodium iodide symporter), member 5	DOWN
1439987_at	Grik1	glutamate receptor, ionotropic, kainate 1	DOWN
1443865_at 1455444_at	Gabra2	gamma-aminobutyric acid (GABA-A) receptor, subunit alpha 2	DOWN
1448788_at	Cd200	CD200 antigen	DOWN
1454770_at	Cckbr	cholecystokinin B receptor	DOWN
1415904_at 1431056_a_at	Lpl	lipoprotein lipase	UP
1417839_at	Cldn5	claudin 5	UP
1418898_at 1423322_at 1449262_s_at 1450937_at	Lin7c	lin-7 homolog C (C. elegans)	UP
Category: mitochondrion			
1431406_at	Agxt2l1	alanine-glyoxylate aminotransferase 2-like 1	DOWN
1439197_at	Pi4kb	phosphatidylinositol 4-kinase, catalytic, beta polypeptide	DOWN
1426387_x_at 1436944_x_at	4933439C20Rik /// LOC236604 /// Pisd	RIKEN cDNA 4933439C20 gene /// phosphatidylserine decarboxylase pseudogene /// phosphatidylserine decarboxylase	UP
1431006_at	Mrpl3	mitochondrial ribosomal protein L3	UP
1431241_at	Chchd3 /// LOC100046321	coiled-coil-helix-coiled-coil-helix domain containing 3 /// similar to coiled-coil-helix-coiled-coil-helix domain containing 3	UP
Category: cytoskeleton			
1421090_at	Epb4.111	erythrocyte protein band 4.1-like 1	DOWN
1435551_at	Fhod3	formin homology 2 domain containing 3	DOWN
1450208_a_at	Elmo1	engulfment and cell motility 1, ced-12 homolog (C. elegans)	DOWN
1455708_at	Tmod3	Tropomodulin 3	DOWN
1420863_at 1458541_at	Dctn4	dynactin 4	UP
Category: extracellular region			
1423286_at 1423287_at	Cbln1 /// LOC100046314	cerebellin 1 precursor protein /// similar to precerebellin-1	DOWN
1433607_at	Cbln4	cerebellin 4 precursor protein	DOWN
1434993_at	B830045N13Rik	RIKEN cDNA B830045N13 gene	DOWN
1434719_at	A2m /// LOC677369	alpha-2-macroglobulin /// hypothetical protein LOC677369	UP
Category: endoplasmic reticulum			

1416507_at	Cnpy2	canopy 2 homolog (zebrafish)	DOWN
1438435_at	Phca	phytoceramidase, alkaline	DOWN
1444037_at	Lman1	lectin, mannose-binding, 1	DOWN
1449859_at	Golt1b	golgi transport 1 homolog B (S. cerevisiae)	DOWN
Category: extracellular space			
1417765_a_at	Amy1	amylase 1, salivary	DOWN
1419426_s_at	100038965 /// Ccl21a /// Ccl21b /// Ccl21c /// ENSMUSG000000073 869 /// LOC100041504 /// LOC100041593 /// LOC100042493 /// OTTMUSG00000011 350	predicted gene, 100038965 /// chemokine (C-C motif) ligand 21a /// chemokine (C-C motif) ligand 21b /// chemokine (C-C motif) ligand 21c (leucine) /// predicted gene, ENSMUSG00000073869 /// similar to beta chemokine Exodus-2 /// similar to beta chemokine Exodus-2 /// similar to beta chemokine Exodus-2 /// predicted gene, OTTMUSG00000011350	DOWN
1417638_at	Lefty1	left right determination factor 1	UP
Category: intracellular			
1449491_at	Card10	caspase recruitment domain family, member 10	DOWN
1456257_at	D1ErtD53e	DNA segment, Chr 1, ERATO Doi 53, expressed	DOWN
1456518_at	4930422I07Rik	RIKEN cDNA 4930422I07 gene	DOWN
Category: cytosol			
1421385_a_at	Myo7a	myosin VIIa	DOWN
1447831_s_at	Mtmr7	myotubularin related protein 7	DOWN
1436991_x_at 1437171_x_at	Gsn	gelsolin	UP
Category: other			
1416953_at	Ctgf	connective tissue growth factor	DOWN
1430485_at	Trpc2	transient receptor potential cation channel, subfamily C, member 2	DOWN
1439650_at	Rtn4	reticulon 4	DOWN
1418687_at	Arc	activity regulated cytoskeletal-associated protein	DOWN
1456685_at	Nsg2	neuron specific gene family member 2	DOWN
1458203_at	Spire1	Spire homolog 1 (Drosophila)	DOWN
1455600_at	Rps3	ribosomal protein S3	DOWN
1449421_a_at	Kcne2	potassium voltage-gated channel, Isk-related subfamily, gene 2	DOWN
1455965_at	Adamts4	a disintegrin-like and metalloproteinase (reprolysin type) with thrombospondin type 1 motif, 4	UP
1442742_at	Atp2c1	ATPase, Casequestering	UP
1434624_x_at	Rps9	ribosomal protein S9	UP
1438936_s_at 1438937_x_at	Ang	angiogenin, ribonuclease, RNase A family, 5	UP
1421144_at	Rpgrip1	retinitis pigmentosa GTPase regulator interacting protein 1	UP

Table S6 Genes whose expression levels are modified in transgenic compared to wild type hippocampus. Clustering according to Gene Ontology (Molecular function)



Probe Set ID	Gen Symbol	Gene Name	Change
Category: protein binding			
1416200_at	Il33	interleukin 33	DOWN
1416250_at 1448272_at	Btg2	B-cell translocation gene 2, anti-proliferative	DOWN
1416507_at	Cnpy2	canopy 2 homolog (zebrafish)	DOWN
1416953_at	Ctgf	connective tissue growth factor	DOWN
1418701_at	Comt1	catechol-O-methyltransferase 1	DOWN
1423129_at 1425845_a_at	Shoc2	soc-2 (suppressor of clear) homolog (C. elegans)	DOWN
1423286_at 1423287_at	Cbln1 /// LOC100046314	cerebellin 1 precursor protein /// similar to precerebellin-1	DOWN
1439650_at	Rtn4	reticulon 4	DOWN
1440142_s_at	Gfap	glial fibrillary acidic protein	DOWN
1441573_at	Scmh1	Sex comb on midleg homolog 1	DOWN
1441684_at	Ttc3	tetratricopeptide repeat domain 3	DOWN
1448229_s_at	Ccnd2	cyclin D2	DOWN

1448788_at	Cd200	CD200 antigen	DOWN
1449030_at	Syn2	synapsin II	DOWN
1449491_at	Card10	caspase recruitment domain family, member 10	DOWN
1450208_a_at	Elmo1	engulfment and cell motility 1, ced-12 homolog (C. elegans)	DOWN
1457751_at	4832420A03Rik /// Rsf1	RIKEN cDNA 4832420A03 gene /// remodeling and spacing factor 1	DOWN
1417839_at	Cldn5	claudin 5	UP
1418898_at 1423322_at 1449262_s_at 1450937_at	Lin7c	lin-7 homolog C (C. elegans)	UP
1420863_at 1458541_at	Dctn4	dynactin 4	UP
1421144_at	Rpgrip1	retinitis pigmentosa GTPase regulator interacting protein 1	UP
1425521_at	Paip1	polyadenylate binding protein-interacting protein 1	UP
1426906_at 1452231_x_at	Ifi203	interferon activated gene 203	UP
1429244_at	1500011B03Rik /// 2610524H06Rik	RIKEN cDNA 1500011B03 gene /// RIKEN cDNA 2610524H06 gene	UP
1434719_at	A2m /// LOC677369	alpha-2-macroglobulin /// hypothetical protein LOC677369	UP
1441955_s_at	LOC676674 /// Paip1	similar to poly(A) binding protein interacting protein 1 /// polyadenylate binding protein-interacting protein 1	UP
1446144_at	Pex5l	peroxisomal biogenesis factor 5-like	UP
1448406_at	Eid1	EP300 interacting inhibitor of differentiation 1	UP
Category: DNA binding			
1419380_at	Zfp423	zinc finger protein 423	DOWN
1428417_at 1428418_s_at	3110050N22Rik	RIKEN cDNA 3110050N22 gene	DOWN
1449490_at	Mbd4	methyl-CpG binding domain protein 4	DOWN
1455246_at	Smarcc1	SWI/SNF related, matrix associated, actin dependent regulator of chromatin, subfamily c, member 1	DOWN
1459372_at	Npas4	neuronal PAS domain protein 4	DOWN
1423477_at	LOC100044533 /// Zic1	similar to Zic protein /// zinc finger protein of the cerebellum 1	UP
1429951_at	Ssbp2	single-stranded DNA binding protein 2	UP
1431213_a_at 1431214_at	LOC433762	hypothetical gene LOC433762	UP
1436994_a_at	Hist1h1c	histone cluster 1, H1c	UP
1439627_at	Zic1	zinc finger protein of the cerebellum 1	UP
Category: transcription factor activity			
1415899_at	Junb	Jun-B oncogene	DOWN
1416505_at	Nr4a1	nuclear receptor subfamily 4, group A, member 1	DOWN

1418174_at 1438211_s_at	Dbp	D site albumin promoter binding protein	DOWN
1421028_a_at 1451507_at	Mef2c	myocyte enhancer factor 2C	DOWN
1421163_a_at	Nfia	nuclear factor I/A	DOWN
1423100_at	Fos	FBJ osteosarcoma oncogene	DOWN
1427682_a_at	Egr2	early growth response 2	DOWN
1443020_at	Hmbox1	homeobox containing 1	DOWN
1459250_at	Tshz2	teashirt zinc finger family member 2	DOWN
Category: actin binding			
1418687_at	Arc	activity regulated cytoskeletal-associated protein	DOWN
1421090_at	Epb4.111	erythrocyte protein band 4.1-like 1	DOWN
1435551_at	Fhod3	formin homology 2 domain containing 3	DOWN
1439397_at	Fmn1	formin 1	DOWN
1455708_at	Tmod3	Tropomodulin 3	DOWN
1458203_at	Spire1	Spire homolog 1 (Drosophila)	DOWN
1417461_at 1417462_at	Cap1	CAP, adenylate cyclase-associated protein 1 (yeast)	UP
1436991_x_at 1437171_x_at	Gsn	gelsolin	UP
1438936_s_at 1438937_x_at	Ang	angiogenin, ribonuclease, RNase A family, 5	UP
Category: ion channel activity			
1421738_at	Gabra2 /// LOC100047443	gamma-aminobutyric acid (GABA-A) receptor, subunit alpha 2 /// similar to Gamma-aminobutyric-acid receptor subunit alpha-2 precursor (GABA(A) receptor subunit alpha-2)	DOWN
1430485_at	Trpc2	transient receptor potential cation channel, subfamily C, member 2	DOWN
1439987_at	Grik1	glutamate receptor, ionotropic, kainate 1	DOWN
1443865_at 1455444_at	Gabra2	gamma-aminobutyric acid (GABA-A) receptor, subunit alpha 2	DOWN
1449421_a_at	Kcne2	potassium voltage-gated channel, Isk-related subfamily, gene 2	DOWN
1450712_at	Kcnj9	potassium inwardly-rectifying channel, subfamily J, member 9	DOWN
1440397_at	Cacna2d1	calcium channel, voltage-dependent, alpha2/delta subunit 1	UP
1456923_at	Trpm3	transient receptor potential cation channel, subfamily M, member 3	UP
Category: nucleic acid binding			
1440125_at 1442654_at	A530054K11Rik	RIKEN cDNA A530054K11 gene	DOWN
1444092_at	9430025M13Rik	RIKEN cDNA 9430025M13 gene	DOWN
1456518_at	4930422I07Rik	RIKEN cDNA 4930422I07 gene	DOWN
1424784_at	OTTMUSG0000 0010657	predicted gene, OTTMUSG00000010657	UP
1429308_at	Prdm16	PR domain containing 16	UP

1434171_at	C330011K17Rik	RIKEN cDNA C330011K17 gene	UP
Category: protein kinase activity			
1422659_at 1427763_a_at	Camk2d	calcium/calmodulin-dependent protein kinase II, delta	DOWN
1429463_at	Prkaa2	protein kinase, AMP-activated, alpha 2 catalytic subunit	DOWN
1435162_at	Prkg2	protein kinase, cGMP-dependent, type II	DOWN
1439843_at 1441974_at	Camk4	calcium/calmodulin-dependent protein kinase IV	DOWN
1440801_s_at	Adrbk2	adrenergic receptor kinase, beta 2	DOWN
1437579_at	Nek2	NIMA (never in mitosis gene a)-related expressed kinase 2	UP
Category: RNA binding			
1431708_a_at	Tia1	cytotoxic granule-associated RNA binding protein 1	DOWN
1455600_at	Rps3	ribosomal protein S3	DOWN
1434624_x_at	Rps9	ribosomal protein S9	UP
1437904_at	Rbm45	RNA binding motif protein 45	UP
Category: signal transducer activity			
1417432_a_at 1454696_at	Gnb1	guanine nucleotide binding protein (G protein), beta 1	DOWN
1421087_at	Per3	period homolog 3 (Drosophila)	DOWN
1449859_at	Golt1b	golgi transport 1 homolog B (S. cerevisiae)	DOWN
1420940_x_at 1420942_s_at	Rgs5	regulator of G-protein signaling 5	UP
Category: calcium ion binding			
1417765_a_at	Amy1	amylase 1, salivary	DOWN
1435400_at	2900075B16Rik	RIKEN cDNA 2900075B16 gene	DOWN
1420429_at	Pcdhb3	protocadherin beta 3	UP
1442742_at	Atp2c1	ATPase, Casequestering	UP
Category: peptidase activity			
1437537_at	Casp9	caspase 9	DOWN
1440413_at	A830006F12Rik	RIKEN cDNA A830006F12 gene	DOWN
1431057_a_at	Prss23	protease, serine, 23	UP
1455965_at	Adamts4	a disintegrin-like and metallopeptidase (reprolysin type) with thrombospondin type 1 motif, 4	UP
Category: kinase activity			
1439197_at	Pi4kb	phosphatidylinositol 4-kinase, catalytic, beta polypeptide	DOWN
1458240_at	Magi1	Membrane associated guanylate kinase, WW and PDZ domain containing 1	DOWN
1439740_s_at	Uck2	uridine-cytidine kinase 2	UP
1455657_at	2610207I05Rik	RIKEN cDNA 2610207I05 gene	UP

Category: nucleotide binding			
1431182_at	EG666031 /// Hspa8 /// LOC624853 /// LOC641192	predicted gene, EG666031 /// heat shock protein 8 /// hypothetical LOC624853 /// similar to heat shock protein 8	DOWN
1454772_at	Ascc3l1	Activating signal cointegrator 1 complex subunit 3-like 1	DOWN
1455136_at	Atp1a2	ATPase, Na ⁺ transporting, alpha 2 polypeptide	DOWN
Category: phosphoprotein phosphatase activity			
1447831_s_at	Mtmr7	myotubularin related protein 7	DOWN
1448830_at	Dusp1	dual specificity phosphatase 1	DOWN
1429691_at	Ptprg	protein tyrosine phosphatase, receptor type, G	UP
Category: structural molecule activity			
1419230_at 1419231_s_at	Krt12	keratin 12	DOWN
1449154_at	Col11a1	collagen, type XI, alpha 1	DOWN
1427883_a_at	Col3a1	collagen, type III, alpha 1	UP
Category: hydrolase activity			
1438435_at	Phca	phytoceramidase, alkaline	DOWN
1415904_at 1431056_a_at	Lpl	lipoprotein lipase	UP
1418148_at	Abhd1	abhydrolase domain containing 1	UP
Category: other			
1423760_at 1434376_at	Cd44	CD44 antigen	DOWN
1454770_at	Cckbr	cholecystokinin B receptor	DOWN
1425029_a_at	Mboat2	membrane bound O-acyltransferase domain containing 2	DOWN
1431406_at	Agxt2l1	alanine-glyoxylate aminotransferase 2-like 1	DOWN
1421385_a_at	Myo7a	myosin VIIa	DOWN
1424877_a_at	Alad /// LOC100046072	aminolevulinatase, delta-, dehydratase /// similar to aminolevulinatase, delta-, dehydratase	DOWN
1436239_at	Slc5a5	solute carrier family 5 (sodium iodide symporter), member 5	DOWN
1446244_at	Zyg11b	zyg-II homolog B (C. elegans)	DOWN
1450779_at	Fabp7	fatty acid binding protein 7, brain	UP
1430979_a_at	Prdx2	peroxiredoxin 2	UP

Table S7 Escape latency on odd trials across the acquisition sessions of the reversal learning paradigm

Session	ANOVA $F_{(1,19)}$	<i>P</i> value
1 odd	22.299	<i>P</i> = 0.000
1 even	6.853	<i>P</i> = 0.017
2 odd	1.681	<i>P</i> = 0.211
2 even	2.999	<i>P</i> = 0.100
3 odd	5.398	<i>P</i> = 0.032
3 even	20.266	<i>P</i> = 0.000
4 odd	7.630	<i>P</i> = 0.013
4 even	6.137	<i>P</i> = 0.023
5 odd	33.608	<i>P</i> = 0.000
5 even	14.924	<i>P</i> = 0.001
6 odd	13.470	<i>P</i> = 0.002
6 even	12.811	<i>P</i> = 0.002
7 odd	15.939	<i>P</i> = 0.001
7 even	12.914	<i>P</i> = 0.002
8 odd	2.242	<i>P</i> = 0.152
8 even	2.060	<i>P</i> = 0.037

P values correspond to ANOVA $F_{(1,19)}$

Table S8 Categorization of activity-dependent genes according to their induction by DREAM derepression and/or the nuclear calcium/calmodulin complex as defined in [1]

(A) DREAM target genes whose activity-dependent induction is independent of the nuclear calcium/calmodulin complex

ID	Symb	tg	Bicc/Inh	Gene Name
NM_009234	Sox11	4.7	**/-	SRY-box containing gene 11
NM_010234	c-Fos	4.2	***/-	FBJ osteosarcoma oncogene
NM_010774	Mbd4	3.1	nc/-	methyl-CpG binding domain protein 4
NM_080455	Tshz2	2.4	nc/-	teashirt zinc finger family member 2
NM_001122952	Nfia	1.9	nc/-	nuclear factor I/A
NM_010118	Egr2	1.8	***/-	early growth response 2
NM_001170537	Mef2c	1.8	nc/-	myocyte enhancer factor 2C
NM_011067	Per3	1.6	nc/-	period homolog 3 (Drosophila)

Column headings are as follows: ID, GenBank identification number; Symb, gene symbol; tg, fold repression in DREAM transgenic hippocampus; Bicc/Inh as defined in [1] Bicc/, change in the expression after biccuculine-induced action potential bursting: nc, no change, ** between 5 and 10 fold and *** more than 10-fold; /Inh, percentage of inhibition of the change following blockade of nuclear calcium signaling with CaMBP4: -, inhibition lower than 40%

(B) Genes that are induced by both DREAM derepression and the nuclear calcium/calmodulin complex

ID	Symb	tg	Bicc/Inh	Gene
NM_153553	Npas4	3.3	***/**	neuronal PAS domain protein 4
NM_026324	Kirrel3	2.8	*/**	Kin of IRRE like 3 (Drosophila)
NM_018790	Arc	2.5	***/**	activity regulated cytoskeletal-associated protein
NM_013642	Dusp1	2.5	**/*	dual specificity phosphatase 1
NM_010444	Nr4a1	2.1	***/*	nuclear receptor subfamily.4, group A, member 1
NM_007570	Btg2	1.8	***/ref	B-cell translocation gene 2
NM_008416	JunB	1.8	***/**	Jun B protooncogene
NM_023324	Peli1	1.8	*/*	pellino 1
	Gadd45			Growth arrest and DNA-damage-inducible 45
NM_008655	b	1.6	***/**	beta
NM_011361	Sgk	1.5	**/*	Serum- glucocorticoid-inducible kinase
NM_028755	Arpp21	1.5	*/*	cyclic AMP-regulated phosphoprotein, 21
BM941356	Pcdh9	1.5	**/**	Protocadherin 9
NM_013613	Nr4a2	1.5	**/*	nuclear receptor subfamily.4, group A, member 2
NM_018820	Sertad1	1.5	**/*	SERTA domain containing 1

Column headings are as follows: ID, GenBank identification number; Symb, gene symbol; tg, Fold repression in DREAM transgenic hippocampus; Bicc/Inh as defined in [1] Bicc/, change in the expression after biccuculine-induced action potential bursting: *, change between 2 and 5 fold, ** between 5 and 10 fold and *** more than 10-fold; /Inh, percentage of inhibition of the change following blockade of nuclear calcium signaling with CaMBP4: *, inhibition between 40 and 60%, ** inhibition between 60 and 80%, *** inhibition greater than 80%

(C) Activity-dependent genes whose induction is not related to DREAM derepression

ID	Symb	tg	Bicc/Inh	Gene
NM_008327	Ifi202b	nc	***/**	interferon activated gene 202B
NM_008380	Inhba	nc	***/**	inhibin beta-A
NM_011111	Serpib2	nc	***/**	serine (or cysteine) peptidase inhibitor, clade B, member 2
NM_025413	Lce1g	nc	***/**	late cornified envelope 1G
NM_011982	Homer	nc	***/**	homer homolog 1 (Drosophila)
NM_011198	Ptgs2	nc	***/**	prostaglandin-endoperoxide synthase 2
NM_007498	Atf3	nc	***/**	activating transcription factor 3
NM_008842	Pim1	nc	***/**	proviral integration site 1
NM_008013	Fgl2	nc	**/**	fibrinogen-like protein 2
BE691546	C030046G05	nc	**/**	
BE956940	Lonrf3	nc	**/**	LON peptidase N-terminal domain and ring finger 3
M13227	Penk	nc	**/**	proenkephalin
NM_010207	Fgfr2	nc	**/**	fibroblast growth factor receptor 2
NM_028760	Cep55	nc	**/**	centrosomal protein 55
NM_029667	Lce1i	nc	**/**	late cornified envelope 1I
NM_172576	Baz1a	nc	**/**	bromodomain adjacent to zinc finger domain 1A
AK004371	Ras11a	nc	**/**	RAS-like, family 11, member A
AW555393	Mest	nc	**/**	mesoderm specific transcript
BE687858	BC023892	nc	**/**	
NM_008872	Plat	nc	**/**	plasminogen activator, tissue
NM_008987	Ptx3	nc	**/**	pentraxin related gene
NM_009044	Rel	nc	**/**	reticuloendotheliosis oncogene
		nc		solute carrier family 2 (facilitated glucose transporter), member 3
NM_010193	Slc2a3		**/**	
NM_021788	Sap30	nc	**/**	sin3 associated polypeptide
NM_027559	BC063749	nc	**/**	
NM_029466	Arl5b	nc	**/**	ADP-ribosylation factor-like 5B
NM_133753	Errfi1	nc	**/**	ERBB receptor feedback inhibitor 1
BM941356	Fbxo33	nc	**/**	F-box protein 33
NM_017373	Nfil3	nc	**/**	nuclear factor, interleukin 3, regulated
NM_144549	Trib1	nc	**/**	tribbles homolog 1 (Drosophila)
NM_145463	Tmem46	nc	**/**	transmembrane protein 46
NM_153287	Axud1	nc	**/**	AXIN1 up-regulated 1

Column headings are as follows: ID, GenBank identification number; Symb, gene symbol; tg, nc, no change in DREAM transgenic hippocampus as compared to wild type; Bicc/Inh as defined in [1] Bicc/, change in the expression after bicuculine-induced action potential bursting: ** change between 5 and 10 fold and *** more than 10-fold; /Inh, percentage of inhibition of the change following blockade of nuclear calcium signaling with CaMBP4: *, inhibition between 40 and 60%, ** inhibition between 60 and 80%, *** inhibition greater than 80%

Reference

1. Zhang SJ, Zou M, Lu L, Lau D, Ditzel DA, Delucinge-Vivier C, Aso Y, Descombes P, Bading H (2009) Nuclear calcium signaling controls expression of a large gene pool: identification of a gene program for acquired neuroprotection induced by synaptic activity. *PLoS Genet* 5 (8):e1000604